Terahertz multichannel microfluidic sensor based on parallel-plate waveguide resonant cavities

Victoria Astley, Kimberly S. Reichel, Jonathan Jones,[a] Rajind Mendis, and Daniel M. Mittleman[b]
Rice University, Department of Electrical and Computer Engineering, MS 378, Houston, Texas 77251-1892, USA

(Received 7 December 2011; accepted 16 May 2012; published online 5 June 2012)

We demonstrate a terahertz multichannel microfluidic sensor based on a parallel-plate waveguide geometry with two independent integrated resonant cavities. The resonant frequency of each cavity exhibits an approximately linear dependence on the index of refraction of the material inside the cavity and each cavity is demonstrated to respond independently with no measurable crosstalk. The sensitivities of the two cavities in terms of the change in resonant wavelength per refractive index unit (RIU) are measured to be 1.21×10^6 nm/RIU and 6.77×10^5 nm/RIU. © *2012 American Institute of Physics*. [http://dx.doi.org/10.1063/1.4724204]

Considerable interest has focused in recent years on developing resonant structures in the terahertz (THz) regime to be employed for sensing applications, particularly microfluidic sensing. For example, resonant structures such as cavities in photonic crystal waveguides,[1,2] asymmetric split-ring resonators,[3] thin metallic meshes[4] and Bragg filters and photonic band gap structures integrated into parallel-plate waveguides (PPWGs)[5,6] have been proposed for sensing applications. On-chip THz devices incorporating ring resonators and band-pass and band-stop filters to measure the properties of very thin dielectric layers have also been demonstrated.[7,8] In previous work, we demonstrated a different kind of resonant structure: a cavity integrated into a PPWG.[9] In this geometry, the resonant cavity is a rectangular groove machined into the lower plate of the waveguide, which acts as a narrow-band filter for terahertz radiation propagating inside the waveguide in the lowest-order transverse-electric (TE_1) mode.[10] This structure acts as a refractive index sensor; when the cavity is filled with a dielectric material, there is a corresponding change in the resonant frequency dependent on the material's refractive index. This geometry has the advantage that it is compatible with liquid flow, and can therefore be implemented easily in microfluidic sensing and real-time flow monitoring applications. However, a key capability for a microfluidics platform is parallelism—the ability to interrogate more than one fluid sample simultaneously and independently.[11] In this work, we demonstrate that our sensing platform can be used for parallel monitoring, by exploiting the broad bandwidth of single-cycle terahertz pulses.

The PPWG microfluidic sensor consists of two polished aluminum plates assembled with a 1 mm plate separation provided by glass spacers. To demonstrate the independence of multiple resonators, two rectangular grooves are machined into the bottom plate of the waveguide perpendicular to the direction of propagation of the terahertz wave. These two grooves have different geometries, which are designed to give rise to independent resonances that are well-separated in frequency and therefore uncoupled. Groove 1, closer to the input face of the waveguide, has a depth of 406 μm and width of 711 μm. Groove 2, located 2.08 mm further from the input face, is narrower than groove 1, with the same depth and a width of 457 μm. This geometry is based on results from finite element method (FEM) simulations,[12] in which we optimized the width of each groove and the separation between them to obtain two resonances well-separated in frequency that each arise from only one of the grooves. The input face of this waveguide is illuminated with pulsed terahertz radiation with the electric field oriented parallel to the plates to excite the TE_1 mode of the waveguide,[9] as required for coupling to this waveguide geometry. The radiation propagates along the waveguide and is collected after it emerges from the output face. A diagram of the waveguide design and experimental setup is shown in Figure 1.

The resonant behavior of this PPWG structure is characterized using a commercial THz time-domain spectroscopy system to obtain the time-domain waveforms, which are then Fourier-transformed and compared to a waveguide without grooves which serves as a reference. A time window of 1550 ps is used to obtain frequency resolution of ~0.6 GHz. These experimental spectra are compared to results from FEM simulations.[12]

The experimental power transmission spectrum for the multichannel PPWG is shown by the black curve in Figure 2(a). The spectrum displays the two resonances, with frequencies of 265 GHz (with a Q-factor of 32) and 290 GHz

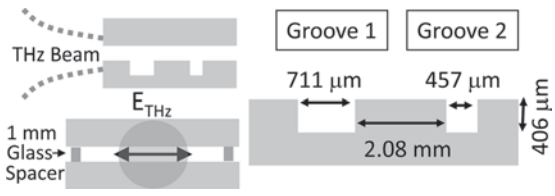

FIG. 1. Diagrams of the PPWG sensor and experimental setup, showing the orientation of the waveguide with respect to the incident THz beam and the geometry of the waveguide and grooves.

[a]Present address: Eastern Illinois University, 600 Lincoln Avenue, Charleston, Illinois 61920-3099, USA.
[b]Author to whom correspondence should be addressed. Electronic mail: daniel@rice.edu.

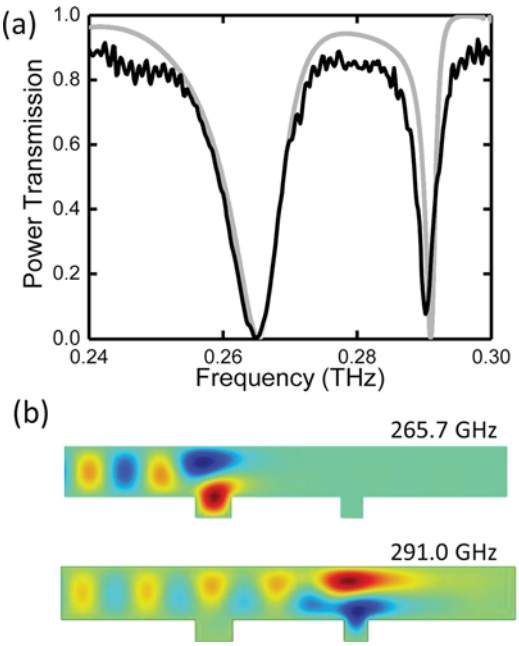

FIG. 2. (a) Power transmission spectra for the empty PPWG sensor, experimental (black curve) and from mode-matching theory (gray curve). The two resonant features arising from the two grooves are clearly visible at 265.0 GHz for groove 1 and 290.2 GHz for groove 2 for the experimental spectrum and at 265.7 GHz and 291.0 GHz for the theoretical case. (b) FEM simulation images of the electric field pattern inside the waveguide at the theoretical resonant frequencies.

($Q = 88$). Over the course of several trials, the standard deviations for these frequencies were $\sigma_1 = 1.65$ GHz and $\sigma_2 = 1.17$ GHz. This variation is most likely due to slight variations in the plate spacing as the waveguide was assembled and disassembled for each trial, with the observed standard deviations corresponding to a variation of $\sim 10\,\mu$m in plate spacing.[13] The gray curve in Figure 2(a) shows the spectrum predicted by mode-matching analysis, with resonant frequencies of 265.7 GHz and 291.0 GHz, within the standard deviations of the measured frequencies. Additionally, electric field patterns obtained from FEM simulation (Fig. 2(b)) illustrate the concentration of energy in each groove at its respective resonant frequency, with little interaction between the two grooves, as needed for independent operation of the two channels.

To establish the capability of this PPWG as a multichannel microfluidic sensor, we test the response of each resonance individually to the presence of a liquid in the associated groove. The liquid test materials were the series of simple straight-chain alkanes from octane (C_8H_{18}, referred to as C8 for simplicity) through hexadecane ($C_{16}H_{34}$, referred to as C16), which have well-established refractive indices in the terahertz range[14] and have been used previously to characterize the performance of the single-channel PPWG microfluidic sensor.[10]

In order to obtain reproducible results, it is important that the groove filling be a carefully controlled process. The grooves are filled with liquid using precision syringes to ensure a consistent volume. In order to find a maximum fill level, the grooves were gradually filled by increments of 0.25 μl for groove 1 and 0.1 μl for groove 2. As volume of liquid in the groove increased, there was initially no change in the resonant behavior until a certain minimum filling level was obtained (approximately 6 μl for groove 1 and 3 μl for groove 2), at which point the resonance begins shifting to lower frequencies. The degree of this resonant shift increases in a roughly linear fashion until the groove begins to overflow and the response saturates. In order to ensure reproducibility and avoid over-filling, we use a consistent volume just below the point of overflow/saturation of 11.5 μl for groove 1 and 8.5 μl for groove 2. To avoid cross-contamination of fluids, a designated syringe was used for each liquid, and then cleaned after use. Each spectrum is compared to one obtained immediately prior with both grooves empty to account for the small variation in the resonant frequencies of the unfilled waveguide as described above. Between each data set the waveguide was disassembled and cleaned using hexane (C_6H_{14}) to remove any residue. The resonance shift caused by the liquid is calculated from the difference in frequency for a particular resonant feature in the filled vs. unfilled groove.

To test the independence of the two channels and refractive-index dependence of the shifts in resonant frequency due to liquid filling, data sets were obtained for several combinations of two fluids in the two grooves, using various alkanes. As an initial test, transmission spectra were compared for three filling scenarios: (1) C14 in both grooves (Fig. 3, light gray curves) (2) C10 in groove 1 and C14 in groove 2 (Fig. 3(a), dark gray), and (3) C14 in groove 1 and C10 in groove 2 (Fig. 3(b), dark gray). In Figure 3, each experimental data set differs only in the filling material of one of the grooves, while each pair of transmission spectra differs only in the frequency of the resonance arising from that groove. This clearly demonstrates the independent nature of the resonances. When the same groove is filled with C14 in two different experimental sets, the resonances overlap with very little variation. Table I illustrates this independence quantitatively by comparing the shifts in resonant frequency

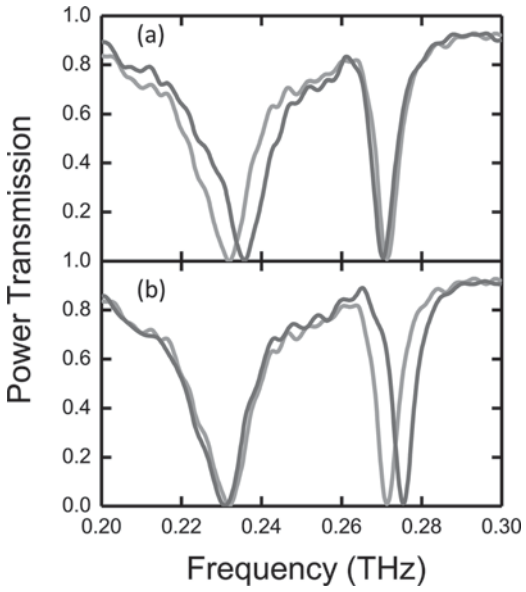

FIG. 3. Power transmission spectra for the PPWG with alkanes filling both grooves. In both plots, light gray curves represent the transmission when both grooves are filled with C14. (a) Dark gray curve: Groove 1 filled with C10 and groove 2 filled with C14. (b) Dark gray curve: Groove 1 filled with C14 and groove 2 filled with C10.

TABLE I. Frequency shifts (relative to the empty waveguide) for the spectra presented in Figure 3.

Material in groove 1	Freq. shift of resonance 1 (GHz)	Material in groove 2	Freq. shift of resonance 2 (GHz)
C10	30.3	C14	20.4
C14	35.0	C14	20.5
C14	35.7	C10	16.6

for each groove and for each alkane fill. The small offset visible in the overlap of the spectra in Figure 3 is a result of the differences in the resonances for the empty PPWG as discussed earlier—the resonance *shifts* are almost identical.

To extend this test, we expand our test liquids to include the full range of alkanes from C8 to C16. For one series of data sets, groove 1 was filled with a substance from the C8 to C16 alkanes, while C14 filled groove 2. By using a consistent substance in one groove, its resonant peak could be monitored to see if it was affected by the filling fluid in the other groove. The same method was applied in a second series of data sets with the constant material, C14, in groove 1 and the range of C8-C16 in groove 2. Figure 4 summarizes these results. We observe that for the groove with the variable liquid filling, the shift in the resonant frequency increases as the refractive index increases, whereas the frequency shift from the groove with a consistent filling material stays constant.

We note that the two grooves have somewhat different sensitivities to small changes in the refractive index of the filling liquid. In particular, the frequency shifts are higher for groove 1 (the larger groove) than for groove 2, although both grooves display a roughly linear relationship between resonant shift and refractive index. Similar to our earlier work,[10] this type of sensor has a high sensitivity as expressed in the resonance shift per refractive index unit (RIU). Using linear fits (dashed lines), for the range of index values spanned by the liquid alkanes the sensitivity is $\Delta f/\Delta n = 225\,\text{GHz/RIU}$ for groove 1 and $\Delta f/\Delta n = 170\,\text{GHz/RIU}$ for groove 2. Converting frequency into wavelength gives a sensitivity of $\Delta\lambda/\Delta n = 1.21 \times 10^6\,\text{nm/RIU}$ for groove 1 and $\Delta\lambda/\Delta n = 6.77 \times 10^5\,\text{nm/RIU}$ for groove 2. These values are slightly higher than the measurement of $3.7 \times 10^5\,\text{nm/RIU}$ for the single-channel sensor, indicating no loss in sensitivity due to multiplexing.[10] These values are more than an order of magnitude higher than the previous highest (theoretical) value reported that of a photonic-crystal-based THz microfluidic sensor.[2] From these sensitivities and the standard deviations of the experimental data (Figure 4, error bars), we estimate the minimum detectable refractive index difference to be $\Delta n \sim 10^{-2}$ RIU, while the theoretical resolution as limited by the spectral resolution of the time-domain THz system (0.6 GHz) would be on the order of 10^{-3} RIU.

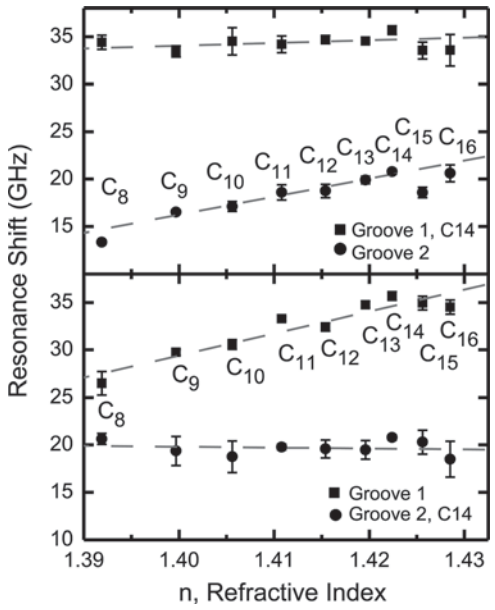

FIG. 4. Plots of the shift in resonant frequency caused by liquid filling in the grooves vs. refractive index of the liquid. In the top plot, groove 1 is consistently filled with C14 while groove 2 is filled with varying alkanes, and the shifts of both resonances are plotted versus the index of the material in groove 2. In the bottom plot, groove 2 is consistently filled with C14 while the material in groove 1 varies and the shifts are plotted versus the index of the material in groove 1. The dotted lines indicate linear fits of the data.

In order for this system to serve as a useful microfluidic sensor, several experimental issues remain to be addressed. The relationships of resonance shift to varying refractive index in the plots above are not precisely linear to within the error bars though they show a clear linear trend, while the "unchanging" resonance does exhibit some fluctuation between the different data sets. These fluctuations in the data could have occurred due to several factors. Since the waveguide is disassembled after each data set for cleaning, it may not be reassembled in exactly the same manner, causing slight variations in the plate spacing and alignment which correspond in turn to slight variations in the observed resonant shift. The effects of evaporation must also be taken into consideration for the lighter alkanes C8, C9, and C10. To minimize evaporation effects a shorter time window was sometimes employed, but this limited the spectral resolution of the measured transmission spectra. In addition, the fill volume must be controlled very carefully and small variations could result in considerable fluctuation in the resonant shift for near-full volumes. These factors will all be important for any industrial or experimental implementation of the PPWG multichannel sensor geometry, particularly the repeatability of the fill volume. Many of these issues could be avoided by including an enclosed liquid channel in the structure, for example, with a thin Teflon cap covering the resonator to prevent evaporation and provide a well-defined fill volume.

Despite these issues of implementation, we have clearly demonstrated several key results: the independent nature of the two resonances, the dependence of each resonance on the refractive index of the filling material of the corresponding groove, and the potential of this design based on two independent resonant cavities integrated into a parallel-plate waveguide for multichannel microfluidic sensing applications.

This project was supported in part by the National Science Foundation and by the Air Force Research Laboratory through the CONTACT program.

[1]C. M. Yee and M. S. Sherwin, Appl. Phys. Lett. **94**, 154104 (2009).
[2]H. Kurt and D. S. Citrin, Appl. Phys. Lett. **87**, 241119 (2005).

[3]C. Debus and P. H. Bolivar, Appl. Phys. Lett. **91**, 184102 (2007).
[4]H. Yoshida, Y. Ogawa, Y. Kawai, S. Hayashi, A. Hayashi, C. Otani, E. Kato, F. Miyamura, and K. Kawase, Appl. Phys. Lett. **91**, 253901 (2007).
[5]S. S. Harsha, N. Laman, and D. Grischkowsky, Appl. Phys. Lett. **94**, 091118 (2009).
[6]M. Nagel, P. H. Bolivar, and H. Kurz, Semicond. Sci. Technol. **20**, S281 (2005).
[7]M. Nagel, P. H. Bolivar, M. Brucherseifer, H. Kurz, A. Bosserhoff, and R. Buttner, Appl. Phys. Lett. **80**, 154 (2002).
[8]C. K. Tiang, J. Cunningham, C. Wood, I. C. Hunter, and A. G. Davies, J. Appl. Phys. **100**, 066105 (2006).
[9]R. Mendis and D. M. Mittleman, Opt. Express **17**, 14839 (2009).
[10]R. Mendis, V. Astley, J. Liu, and D. M. Mittleman, Appl. Phys. Lett. **95**, 171113 (2009).
[11]S. B. Cheng, C. D. Skinner, J. Taylor, S. Attiya, W. E. Lee, G. Picelli, and D. J. Harrison, Anal. Chem. **73**, 1472 (2001).
[12]J. Deibel, M. Escarra, N. Berndsen, K. Wang, and D. M. Mittleman, Proc. IEEE **95**, 1624 (2007).
[13]V. Astley, B. McCracken, R. Mendis, and D. M. Mittleman, Opt. Lett. **36**, 1452 (2011).
[14]J. Laib and D. M. Mittleman, J. Infrared Millim. Terahertz Waves **31**, 1015 (2010).